

# Formation of Rust During the Corrosion of Steel in Water and (NH<sub>4</sub>)<sub>2</sub>S<sub>0</sub>4 Solutions

---

Musić, Svetozar; Dragičević, Dragica; Popović, Stanko

Source / Izvornik: **Croatica Chemica Acta, 1993, 66, 469 - 478**

Journal article, Published version

Rad u časopisu, Objavljena verzija rada (izdavačev PDF)

Permanent link / Trajna poveznica: <https://um.nsk.hr/um:nbn:hr:217:226998>

Rights / Prava: [In copyright](#)/[Zaštićeno autorskim pravom.](#)

Download date / Datum preuzimanja: **2025-02-03**



Repository / Repozitorij:

[Repository of the Faculty of Science - University of Zagreb](#)



## Formation of Rust During the Corrosion of Steel in Water and $(\text{NH}_4)_2\text{SO}_4$ Solutions

Svetozar Musić<sup>a,\*</sup>, Đurđica Dragčević<sup>a</sup> and Stanko Popović<sup>b</sup>

<sup>a</sup> Ruđer Bošković Institute, P. O. Box 1016,  
41001 Zagreb, Republic of Croatia

<sup>b</sup> Department of Physics, Faculty of Science, University of Zagreb,  
P. O. Box 162, 41001 Zagreb, Republic of Croatia

Received May 25, 1993

Formation of rust during the corrosion of steel in water and  $(\text{NH}_4)_2\text{SO}_4$  solutions was monitored at 20 °C up to 3 months and at 90 °C up to 3 days. All corrosion products were analyzed by X-ray diffraction and Fourier transform IR spectroscopy. Four oxide phases, lepidocrocite ( $\gamma\text{-FeOOH}$ ), goethite ( $\alpha\text{-FeOOH}$ ), magnetite ( $\text{Fe}_3\text{O}_4$ ) and hematite ( $\alpha\text{-Fe}_2\text{O}_3$ ), were found in the corrosion products. Their distribution or absence of some oxide phases in corrosion products were strongly dependent on the experimental conditions. The strong influence of  $(\text{NH}_4)_2\text{SO}_4$  electrolyte on the phase composition of the rust was explained by the cumulative effect of two aggressive ions,  $\text{NH}_4^+$  and  $\text{SO}_4^{2-}$ . Possible pathways for the formation of iron oxide phases in the rust were discussed.

### INTRODUCTION

The phase composition of the corrosion products of steel, formed in aqueous medium, depends on different factors, such as the electrolyte character of aqueous medium, temperature, pH, oxygen content as well as the nature of steel. Surface pretreatment of steel may also affect the phase composition of the corrosion products of steel. In the literature, there are abundant data about the phase composition of the rust formed by the corrosion of steel in aqueous medium. However, discrepancies concerning the chemical and structural properties of the rust are significant. Several factors are responsible for this, such as crystallinity, stoichiometry, particle size of oxide components in the rust, *etc.* Limitations of experimental techniques can also be a source of errors in determination of the phase composition of the rust. Finally, many researchers performed their experiments under poorly defined conditions.

\* Author to whom correspondence should be addressed.

Numerous investigations showed the presence of different oxide phases in the rust, such as  $\text{Fe}(\text{OH})_2$ , amorphous  $\text{Fe}(\text{OH})_3$ , ferrihydrite,  $\alpha\text{-FeOOH}$ ,  $\beta\text{-FeOOH}$ ,  $\gamma\text{-FeOOH}$ ,  $\delta\text{-FeOOH}$ ,  $\alpha\text{-Fe}_2\text{O}_3$ ,  $\gamma\text{-Fe}_2\text{O}_3$  and  $\text{Fe}_3\text{O}_4$  or  $\text{Fe}_{3-x}\text{O}_4$ . In previous papers, we showed that Mössbauer spectroscopy can be a very useful technique in the phase analysis of the rust formed by the atmospheric corrosion of steel<sup>1</sup> or by the corrosion of steel in aqueous medium.<sup>2</sup> The corrosion of steel in aqueous medium is a process of electrochemical nature and the generated rust is a mixture of different oxide phases exhibiting colloidal properties. The mechanism of rust formation during the corrosion of steel in aqueous medium can be followed, to a certain stage, by analogy to the precipitation of iron oxyhydroxides and oxides from  $\text{Fe}(\text{II})$ - or  $\text{Fe}(\text{III})$ -salt solutions.<sup>3-6</sup> The usefulness of these investigations increases as the conditions in the laboratory experiments approach those in actual corrosion processes.

In the present paper, we report the results of the analysis of the corrosion products of steel formed in doubly distilled water and in  $(\text{NH}_4)_2\text{SO}_4$  solutions. These experiments were performed in order to find out the influence of the  $(\text{NH}_4)_2\text{SO}_4$  electrolyte and its concentration on the chemical and structural properties of the rust. X-ray diffraction (XRD) and Fourier transform infrared (FT-IR) spectroscopy were used as instrumental techniques. FT-IR spectroscopy is a technique that is characterized by a better sensitivity and resolution than conventional IR spectroscopy.

TABLE I

*Experimental conditions for the preparation of the corrosion products of steel (samples C<sub>1</sub> to C<sub>24</sub>)*

| Sample          | Solution                           | Temperature of solution (°C) | Time of corrosion* | pH of mother liquor |
|-----------------|------------------------------------|------------------------------|--------------------|---------------------|
| C <sub>1</sub>  | H <sub>2</sub> O                   | 20                           | 1d                 | 5.50                |
| C <sub>2</sub>  | H <sub>2</sub> O                   | 20                           | 3d                 | 5.35                |
| C <sub>3</sub>  | H <sub>2</sub> O                   | 20                           | 7d                 | 5.50                |
| C <sub>4</sub>  | H <sub>2</sub> O                   | 20                           | 21d                | 5.40                |
| C <sub>5</sub>  | H <sub>2</sub> O                   | 20                           | 3m                 | 5.90                |
| C <sub>6</sub>  | H <sub>2</sub> O                   | 90                           | 5h                 | 7.78                |
| C <sub>7</sub>  | H <sub>2</sub> O                   | 90                           | 1d                 | 6.45                |
| C <sub>8</sub>  | H <sub>2</sub> O                   | 90                           | 3d                 | 6.35                |
| C <sub>9</sub>  | 0.1 M $(\text{NH}_4)_2\text{SO}_4$ | 20                           | 1d                 | 7.15                |
| C <sub>10</sub> | 0.1 M $(\text{NH}_4)_2\text{SO}_4$ | 20                           | 3d                 | 7.45                |
| C <sub>11</sub> | 0.1 M $(\text{NH}_4)_2\text{SO}_4$ | 20                           | 7d                 | 7.35                |
| C <sub>12</sub> | 0.1 M $(\text{NH}_4)_2\text{SO}_4$ | 20                           | 21d                | 7.40                |
| C <sub>13</sub> | 0.1 M $(\text{NH}_4)_2\text{SO}_4$ | 20                           | 3m                 | 7.70                |
| C <sub>14</sub> | 0.1 M $(\text{NH}_4)_2\text{SO}_4$ | 90                           | 5h                 | 7.45                |
| C <sub>15</sub> | 0.1 M $(\text{NH}_4)_2\text{SO}_4$ | 90                           | 1d                 | 7.35                |
| C <sub>16</sub> | 0.1 M $(\text{NH}_4)_2\text{SO}_4$ | 90                           | 3d                 | 7.50                |
| C <sub>17</sub> | 2 M $(\text{NH}_4)_2\text{SO}_4$   | 20                           | 1d                 | 7.85                |
| C <sub>18</sub> | 2 M $(\text{NH}_4)_2\text{SO}_4$   | 20                           | 3d                 | 7.90                |
| C <sub>19</sub> | 2 M $(\text{NH}_4)_2\text{SO}_4$   | 20                           | 7d                 | 8.25                |
| C <sub>20</sub> | 2 M $(\text{NH}_4)_2\text{SO}_4$   | 20                           | 21d                | 8.05                |
| C <sub>21</sub> | 2 M $(\text{NH}_4)_2\text{SO}_4$   | 20                           | 3m                 | 6.80                |
| C <sub>22</sub> | 2 M $(\text{NH}_4)_2\text{SO}_4$   | 90                           | 5h                 | 8.00                |
| C <sub>23</sub> | 2 M $(\text{NH}_4)_2\text{SO}_4$   | 90                           | 1d                 | 7.95                |
| C <sub>24</sub> | 2 M $(\text{NH}_4)_2\text{SO}_4$   | 90                           | 3d                 | 8.00                |

\* h = hour, d = day, m = month

## EXPERIMENTAL

Ammonium sulphate *p. a.*, obtained by Kemika (Zagreb, Croatia) and doubly distilled water were used. Cold rolled low carbon steel, JUS-C0146 ( $C_{\max} = 0.12\%$ ,  $Mn_{\max} = 0.50\%$ ,  $P_{\max} = 0.040\%$ ,  $S_{\max} = 0.040\%$ ), was used. Commercial steel foil was cut into coupons with 60 mm x 100 mm dimensions. The steel coupons were polished and cleaned with doubly distilled water and ethanol. Experiments were performed at 20 or 90 °C. At 20 °C, glass beakers were covered hermetically with polyethylene foils to prevent direct contact of the corrosion system with atmospheric oxygen. In glass beakers, the steel coupons were completely immersed into the aqueous medium. Corrosion of steel at 90 °C was performed in an autoclave. Experimental conditions for the preparation of corrosion products of steel,  $C_1$  to  $C_{24}$ , are given in Table I. Isolated corrosion products were cleaned from mother liquor with doubly distilled water. Sorvall RC2-B ultraspeed centrifuge (up to 20000 r.p.m.) was used for separation of the solid from the liquid phases. The corrosion products were dried in vacuum at room temperature. pH measurements were performed with a pHM-26 instrument and the corresponding electrodes produced by Radiometer. X-ray powder diffraction measurements were performed using a Phillips counter diffractometer with monochromatized  $CuK\alpha$  radiation and graphite monochromator. FT-IR spectra were recorded using a 1720x spectrometer produced by Perkin-Elmer. FT-IR spectrometer was coupled with a personal computer loaded with IR Data Manager (IRDM) program. The samples were pressed into discs using spectroscopically pure KBr. The origin of standard iron oxides was described in a previous paper.<sup>4</sup>

## RESULTS

Phase compositions of the corrosion products formed in doubly distilled water were strongly dependent on the temperature in the experiment. Table II shows the phase composition of the samples, determined by XRD.  $\gamma$ -FeOOH was the dominant component in samples  $C_1$  to  $C_5$ , which were obtained at 20 °C.  $Fe_3O_4$  was an additional component in these samples and the content of  $Fe_3O_4$  in the rust increased with prolonged time of corrosion. FT-IR spectra of samples  $C_1$  to  $C_5$  are shown in Figure 1. Sharp and very pronounced bands at 1024 and 745–750  $cm^{-1}$  are typical of  $\gamma$ -FeOOH. In sample  $C_1$ ,  $Fe_3O_4$  could be detected only on the basis of the shoulder at 549  $cm^{-1}$ . As  $Fe_3O_4$  content increased, the intensity of this shoulder also increased and it was shifted to 557  $cm^{-1}$  for sample  $C_5$ . In sample  $C_5$ , a small amount of  $\alpha$ -FeOOH was also detected by FT-IR, on the basis of bands of very small intensities at 893 and 801  $cm^{-1}$ .

Corrosion of steel in doubly distilled water at 90 °C generated corrosion products in which  $Fe_3O_4$  was the dominant component, while  $\gamma$ -FeOOH and  $\alpha$ - $Fe_2O_3$  were additional components, as shown by XRD analysis (Table II). FT-IR spectra of samples  $C_6$  to  $C_8$  are shown in Figure 2. The  $Fe_3O_4$  component could be detected only on the basis of a very strong band at 575–578  $cm^{-1}$ . However, in the interpretation of these spectra we must keep in mind the fact that this IR band is a superposition of two bands corresponding to both  $Fe_3O_4$  and  $\alpha$ - $Fe_2O_3$ . For this reason, a clear distinction between  $Fe_3O_4$  and  $\alpha$ - $Fe_2O_3$  in these samples was not possible only by FT-IR for the given range, 1400–370  $cm^{-1}$ . The nature of IR bands, corresponding to iron hydroxides, oxyhydroxides, oxides and basic sulphates, was discussed in our previous papers,<sup>7-9</sup> and will not be elaborated in the present paper. FT-IR spectra, shown in Figure 2, also indicated that the content of  $\gamma$ -FeOOH in the rust decreased from sample  $C_6$  to sample  $C_8$ . In sample  $C_8$ , only a small amount of  $\gamma$ -FeOOH could be detected on the basis of a very weak peak at 1021  $cm^{-1}$ . In sample  $C_6$ , a small amount of  $\alpha$ -FeOOH was detected on the basis of bands at 893 and 800  $cm^{-1}$ . With a prolonged time of corrosion, the intensities of these bands were increased.

TABLE II

The result of XRD phase analysis of the corrosion products generated in water and  $(\text{NH}_4)_2\text{SO}_4$  solutions (samples C<sub>1</sub> to C<sub>24</sub>)

| Sample          | Phase composition (approximate molar fraction)  |
|-----------------|---|
| C <sub>1</sub>  | $\gamma\text{-FeOOH} + \text{Fe}_3\text{O}_4$<br>(1/8)  |
| C <sub>2</sub>  | $\gamma\text{-FeOOH} + \text{Fe}_3\text{O}_4$<br>(1/6)  |
| C <sub>3</sub>  | $\gamma\text{-FeOOH} + \text{Fe}_3\text{O}_4$<br>(1/5)  |
| C <sub>4</sub>  | $\gamma\text{-FeOOH} + \text{Fe}_3\text{O}_4$<br>(1/4)  |
| C <sub>5</sub>  | $\gamma\text{-FeOOH} + \text{Fe}_3\text{O}_4$<br>(1/4)  |
| C <sub>6</sub>  | $\text{Fe}_3\text{O}_4 + \gamma\text{-FeOOH} + \alpha\text{-Fe}_2\text{O}_3$<br>(1/8) (1/20)  |
| C <sub>7</sub>  | $\text{Fe}_3\text{O}_4 + \gamma\text{-FeOOH} + \alpha\text{-Fe}_2\text{O}_3$<br>(1/8) (1/20)  |
| C <sub>8</sub>  | $\text{Fe}_3\text{O}_4 + \alpha\text{-Fe}_2\text{O}_3 + \gamma\text{-FeOOH}$<br>(1/10) (1/20) |
| C <sub>9</sub>  | $\gamma\text{-FeOOH}$   |
| C <sub>10</sub> | $\gamma\text{-FeOOH}$   |
| C <sub>11</sub> | $\gamma\text{-FeOOH}$   |
| C <sub>12</sub> | $\gamma\text{-FeOOH} + \text{Fe}_3\text{O}_4$<br>(1/8)  |
| C <sub>13</sub> | $\text{Fe}_3\text{O}_4 + \gamma\text{-FeOOH} + \alpha\text{-FeOOH}$<br>(1/4) (1/4)            |
| C <sub>14</sub> | $\alpha\text{-FeOOH} + \alpha\text{-Fe}_2\text{O}_3 + \text{Fe}_3\text{O}_4$<br>(1/10) (1/10) |
| C <sub>15</sub> | $\alpha\text{-FeOOH} + \alpha\text{-Fe}_2\text{O}_3 + \text{Fe}_3\text{O}_4$<br>(1/10) (1/10) |
| C <sub>16</sub> | $\alpha\text{-FeOOH} + \alpha\text{-Fe}_2\text{O}_3 + \text{Fe}_3\text{O}_4$<br>(1/4) (1/8)   |
| C <sub>17</sub> | $\gamma\text{-FeOOH}^*$   |
| C <sub>18</sub> | $\gamma\text{-FeOOH}^*$   |
| C <sub>19</sub> | $\gamma\text{-FeOOH}^*$   |
| C <sub>20</sub> | $\gamma\text{-FeOOH}^*$   |
| C <sub>21</sub> | $\gamma\text{-FeOOH}$   |
| C <sub>22</sub> | $\alpha\text{-Fe}_2\text{O}_3 + \gamma\text{-FeOOH}$<br>(1/3)                                 |
| C <sub>23</sub> | $\alpha\text{-Fe}_2\text{O}_3 + \gamma\text{-FeOOH}$<br>(1/10)                                |
| C <sub>24</sub> | $\alpha\text{-Fe}_2\text{O}_3 + \alpha\text{-FeOOH} + \gamma\text{-FeOOH}$<br>(1/10) (1/20)   |

\* Broadened diffraction lines

Remark: A small amorphous fraction may be a present in early stages of corrosion.

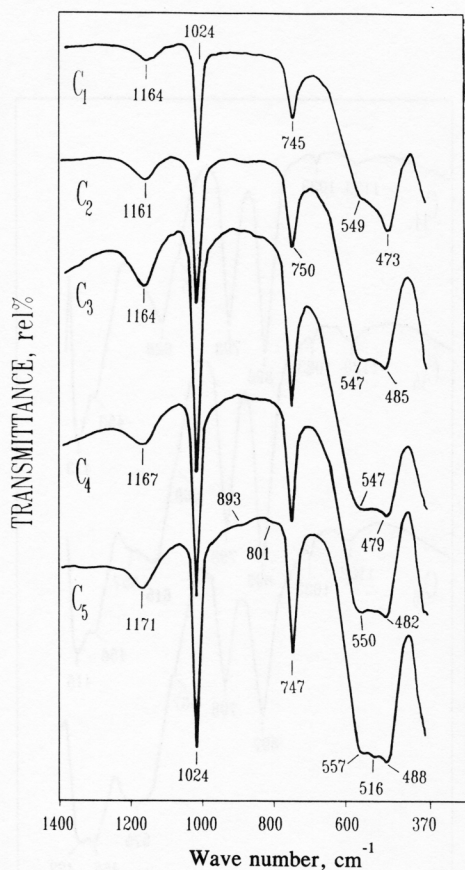


Figure 1. Fourier transform IR spectra of corrosion products  $C_1$  to  $C_5$ , recorded at room temperature.

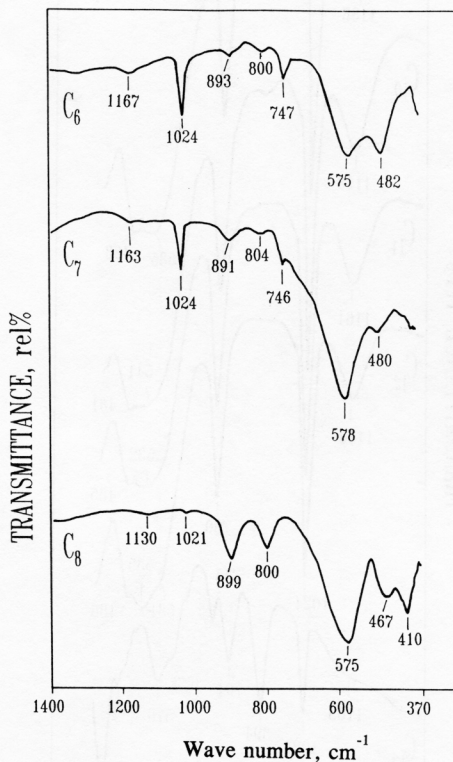


Figure 2. Fourier transform IR spectra of corrosion products  $C_6$  to  $C_8$ , recorded at room temperature.

Corrosion of steel in 0.1 M  $(\text{NH}_4)_2\text{SO}_4$  solution at 20 °C, between 1 and 7 days, generated  $\gamma$ -FeOOH as a single phase in the rust (samples  $C_9$  to  $C_{11}$ ), as shown by XRD (Table II). After 21 days of corrosion,  $\text{Fe}_3\text{O}_4$  was detected by XRD as an additional component (sample  $C_{12}$ ), while after 3 months of corrosion, besides  $\text{Fe}_3\text{O}_4$ ,  $\gamma$ -FeOOH and  $\alpha$ -FeOOH were present (sample  $C_{13}$ ). FT-IR spectroscopic results obtained for samples  $C_9$  to  $C_{13}$  (Figure 3) are in accordance with XRD results. A different phase composition of the rust was obtained when the corrosion of steel in 0.1 M  $(\text{NH}_4)_2\text{SO}_4$  solution was performed at 90 °C. XRD analysis of samples  $C_{14}$  to  $C_{16}$  indicated that  $\alpha$ -FeOOH was the dominant component in these samples, while  $\alpha$ - $\text{Fe}_2\text{O}_3$  and  $\text{Fe}_3\text{O}_4$  were determined as additional components (Table II). FT-IR spectra of samples  $C_{14}$  to  $C_{16}$  (Figure 4) also showed that  $\alpha$ -FeOOH prevailed in these samples, according to the bands at 896 and 798  $\text{cm}^{-1}$ . A very weak peak at 1023–1022  $\text{cm}^{-1}$ , due to a small amount of  $\gamma$ -FeOOH, was observed in FT-IR spectra of samples  $C_{14}$  to  $C_{16}$ .

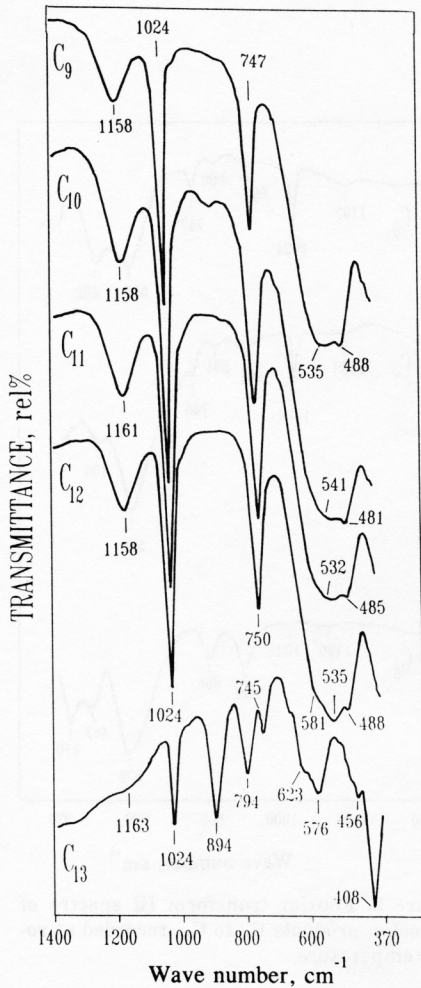


Figure 3. Fourier transform IR spectra of corrosion products  $C_9$  to  $C_{13}$ , recorded at room temperature.

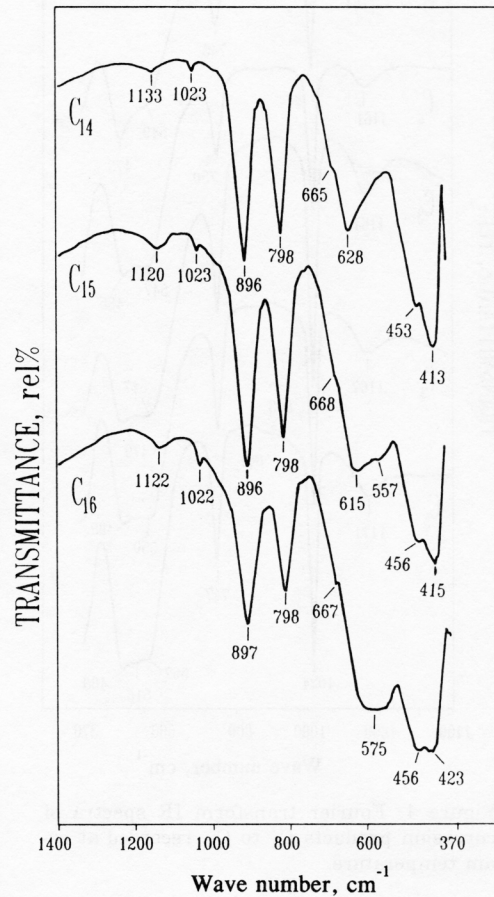


Figure 4. Fourier transform IR spectra of corrosion products  $C_{14}$  to  $C_{16}$ , recorded at room temperature.

Corrosion of steel in 2 M  $(\text{NH}_4)_2\text{SO}_4$  solution at 20 °C, up to 3 months, generated  $\gamma$ -FeOOH as a single phase, samples  $C_{17}$  to  $C_{21}$ , (Table II). XRD lines of  $\gamma$ -FeOOH in samples  $C_{17}$  to  $C_{20}$  were broadened. FT-IR spectra of samples  $C_{17}$  to  $C_{21}$ , shown in Figure 5, also indicated the presence of  $\gamma$ -FeOOH. The presence of a small amount of  $\alpha$ -FeOOH in sample  $C_{21}$  could be recognized on the basis of a band at 895  $\text{cm}^{-1}$  and a shoulder at 795  $\text{cm}^{-1}$ .

After corrosion of steel in 2 M  $(\text{NH}_4)_2\text{SO}_4$  solutions at 90 °C, up to 3 days,  $\alpha$ -Fe $_2$ O $_3$  was determined by XRD as the main component and  $\gamma$ -FeOOH as an additional com-

ponent (samples  $C_{22}$  to  $C_{24}$ ). XRD also showed the presence of  $\alpha$ -FeOOH in sample  $C_{24}$ . FT-IR spectra of samples  $C_{22}$  to  $C_{23}$  are shown in Figure 6. On the basis of very strong bands at  $537$ – $550$   $\text{cm}^{-1}$  and  $473$ – $471$   $\text{cm}^{-1}$ , it was confirmed that  $\alpha$ -Fe $_2$ O $_3$  is the dominant component in the rust. In sample  $C_{22}$ , the presence of  $\gamma$ -FeOOH was detected on the basis of bands at  $1024$  and  $744$   $\text{cm}^{-1}$ , while  $\alpha$ -FeOOH was detected on the basis of a band at  $885$   $\text{cm}^{-1}$  and a shoulder at  $794$   $\text{cm}^{-1}$ . With increased time of corrosion, the intensities of the bands at  $1024$  and  $747$   $\text{cm}^{-1}$ , corresponding to  $\gamma$ -FeOOH, were decreased. In samples  $C_{23}$  and  $C_{24}$ ,  $\alpha$ -FeOOH was detected on the basis of bands at  $896$  and  $800$   $\text{cm}^{-1}$ , and  $898$  and  $802$   $\text{cm}^{-1}$ , respectively.

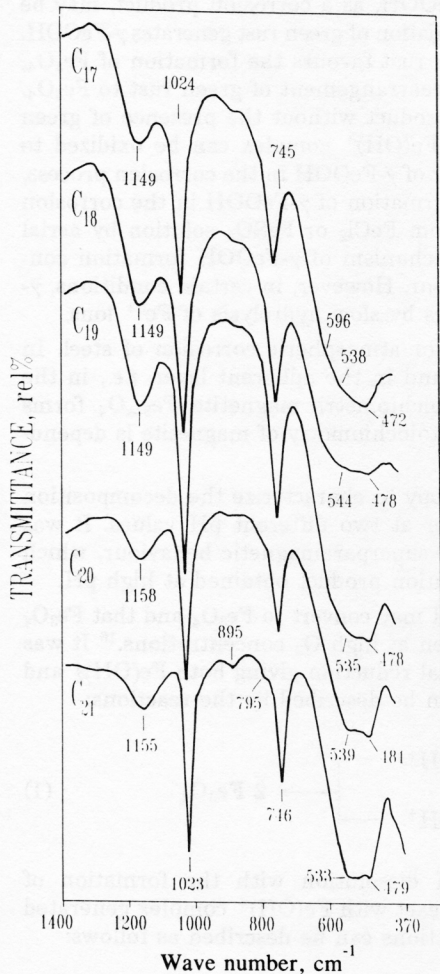


Figure 5. Fourier transform IR spectra of corrosion products  $C_{17}$  to  $C_{21}$ , recorded at room temperature.

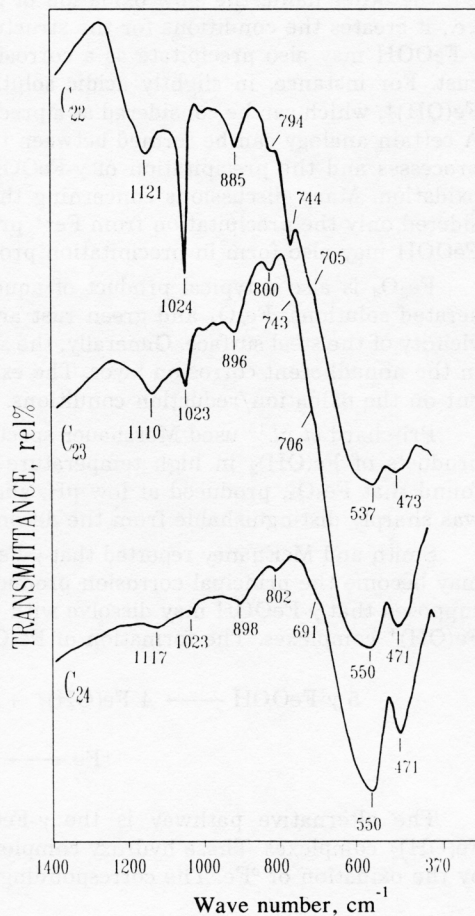


Figure 6. Fourier transform IR spectra of corrosion products  $C_{22}$  to  $C_{24}$ , recorded at room temperature.



## DISCUSSION

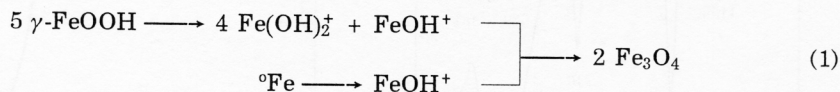
In the present work, four oxide phases, lepidocrocite ( $\gamma$ -FeOOH), goethite ( $\alpha$ -FeOOH), magnetite ( $\text{Fe}_3\text{O}_4$ ) and hematite ( $\alpha$ - $\text{Fe}_2\text{O}_3$ ), were found in corrosion products. Their distribution or absence of some oxide phases in the corrosion products were dependent on the experimental conditions of the corrosion of steel. The experiments performed at 20 °C clearly demonstrated regularities in the phase composition of corrosion products.  $\gamma$ -FeOOH was the dominant component in the rust in all samples obtained at 20 °C, except for sample C<sub>13</sub>, where  $\text{Fe}_3\text{O}_4$  was dominant. Also, all samples, generated in doubly distilled water at 20 °C, up to 3 months, contained  $\text{Fe}_3\text{O}_4$ , while for the same corrosion times in the samples generated in 2 M  $(\text{NH}_4)_2\text{SO}_4$  solution  $\text{Fe}_3\text{O}_4$  was not observed.

Many researchers found  $\gamma$ -FeOOH in the rust, particularly in the rust formed in early stages of the corrosion process.<sup>1,10-14</sup>  $\gamma$ -FeOOH, as a corrosion product, may be formed by different pathways. The rapid aerial oxidation of green rust generates  $\gamma$ -FeOOH. On the other hand, the slow oxidation of green rust favours the formation of  $\text{Fe}_3\text{O}_4$ , *i.e.*, it creates the conditions for the structural rearrangement of green rust to  $\text{Fe}_3\text{O}_4$ .  $\gamma$ -FeOOH may also precipitate as a corrosion product without the presence of green rust. For instance, in slightly acidic solution,  $\text{Fe}(\text{OH})^+$  complex can be oxidized to  $\text{Fe}(\text{OH})_2^+$ , which can be considered as a precursor of  $\gamma$ -FeOOH in the corrosion process. A certain analogy can be formed between the formation of  $\gamma$ -FeOOH in the corrosion processes and the precipitation of  $\gamma$ -FeOOH from  $\text{FeCl}_2$  or  $\text{FeSO}_4$  solution by aerial oxidation. Many discussions concerning the mechanism of  $\gamma$ -FeOOH formation considered only the precipitation from  $\text{Fe}^{2+}$  precursor. However, in certain conditions,  $\gamma$ -FeOOH may also form in precipitation processes by slow hydrolysis of  $\text{Fe}^{3+}$  ions.

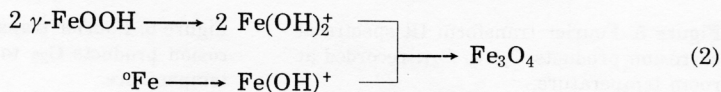
$\text{Fe}_3\text{O}_4$  is also a typical product of aqueous or atmospheric corrosion of steel. In aerated solutions,  $\text{Fe}_3\text{O}_4$  and green rust are found in the adherent layer, *i.e.*, in the vicinity of the steel surface. Generally, the substoichiometric magnetite,  $\text{Fe}_{3-x}\text{O}_4$ , forms in the nonadherent corrosion layer. The exact stoichiometry of magnetite is dependent on the oxidation/reduction conditions.

Pritchard *et al.*<sup>15</sup> used Mössbauer spectroscopy to characterize the decomposition products of  $\text{Fe}(\text{OH})_2$  in high temperature water at two different pH values. It was found that  $\text{Fe}_3\text{O}_4$ , produced at low pH, showed superparamagnetic behaviour, which was sharply distinguishable from the decomposition product obtained at high pH.

Smith and McEnaney reported that  $\gamma$ -FeOOH may convert to  $\text{Fe}_3\text{O}_4$  and that  $\text{Fe}_3\text{O}_4$  may become the principal corrosion product even at high  $\text{O}_2$  concentrations.<sup>16</sup> It was supposed that  $\gamma$ -FeOOH may dissolve with partial reduction giving both  $\text{Fe}(\text{OH})_2^+$  and  $\text{Fe}(\text{OH})^+$  complexes. The formation of  $\text{Fe}_3\text{O}_4$  can be described by the reactions:



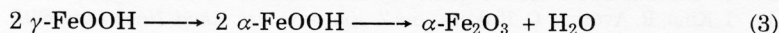
The alternative pathway is the  $\gamma$ -FeOOH dissolution with the formation of  $\text{Fe}(\text{OH})_2^+$  complexes. These hydroxy complexes react with  $\text{Fe}(\text{OH})^+$  complex generated by the oxidation of  $\text{}^0\text{Fe}$ . The corresponding reactions can be described as follows:



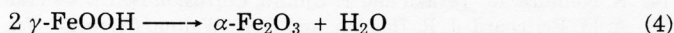
Kassim *et al.*<sup>17</sup> found that the initial corrosion product of iron in aqueous environment was the green rust, which converted to  $\gamma$ -FeOOH or  $\text{Fe}_3\text{O}_4$  depending on the oxidation rate, as well as on the concentration of dissolved oxygen. The transformation of the green rust to the  $\text{Fe}_3\text{O}_4$  was explained by the solid state transformation. The process of transformation  $\gamma$ -FeOOH  $\longrightarrow$   $\text{Fe}_3\text{O}_4$  was also simulated by electrochemical methods.<sup>18,19</sup>

The strong influence of  $(\text{NH}_4)_2\text{SO}_4$  electrolyte on the formation of the rust and its phase composition can be considered as a cumulative effect of two aggressive ions,  $\text{NH}_4^+$  and  $\text{SO}_4^{2-}$ . The presence of  $\text{SO}_4^{2-}$  ions, at given pH values, can create corrosion conditions that show a certain analogy with the processes of precipitation of iron oxyhydroxides and oxides from  $\text{FeSO}_4$  solutions. On the other hand, the presence of  $\text{NH}_4^+$  ions may promote the dissolution of iron (steel) into the solution,<sup>20</sup> thus accelerating the corrosion reactions. In 2 M  $(\text{NH}_4)_2\text{SO}_4$  solution,  $\text{Fe}_3\text{O}_4$  was not formed, even after 3 months of corrosion, in spite of the fact that pH conditions (Table I) favoured the formation of  $\text{Fe}_3\text{O}_4$ .

In the rust formed in  $(\text{NH}_4)_2\text{SO}_4$  solutions at room temperature, no significant amount of  $\alpha$ -FeOOH was found. However, an opposite situation was found in the rust samples obtained at 90 °C, for instance in samples C<sub>14</sub> to C<sub>16</sub>. According to the analysis of the rust, it may be concluded that  $\gamma$ -FeOOH is the main source of material for the formation of  $\alpha$ -FeOOH. Very probably, this transformation occurred by a dissolution/reprecipitation mechanism. Generally, the transformation of  $\gamma$ -FeOOH to  $\alpha$ -FeOOH and  $\alpha$ -Fe<sub>2</sub>O<sub>3</sub> can be expressed by the reactions:



and



At room temperature, the nucleation of  $\alpha$ -FeOOH is easier than that of  $\alpha$ -Fe<sub>2</sub>O<sub>3</sub>. With increase of temperature of aqueous medium the appearance of  $\alpha$ -Fe<sub>2</sub>O<sub>3</sub> in the rust is more probable and this effect is observed in the present study. At 90 °C, all corrosion reactions are very accelerated. The formation of  $\alpha$ -FeOOH in a more significant amount at 90 °C, than at 20 °C, can be explained by an increased rate of  $\gamma$ -FeOOH dissolution and increased concentration of  $\text{Fe}^{3+}$  ions.

## CONCLUSION

Four oxide phases, lepidocrocite ( $\gamma$ -FeOOH), goethite ( $\alpha$ -FeOOH), magnetite ( $\text{Fe}_3\text{O}_4$ ) and hematite ( $\alpha$ -Fe<sub>2</sub>O<sub>3</sub>) were detected in the corrosion products formed by the corrosion of steel in doubly distilled water or  $(\text{NH}_4)_2\text{SO}_4$  solutions. Their distribution or absence of some oxide phases in the corrosion products were dependent on the concentration of  $(\text{NH}_4)_2\text{SO}_4$  solution, the temperature and the time of corrosion. Fourier transform IR spectroscopy, which was used as a complementary technique to X-ray diffraction, was particularly useful in detection of small amounts of  $\gamma$ -FeOOH and  $\alpha$ -FeOOH.  $\gamma$ -FeOOH was the dominant component in all corrosion products obtained at 20 °C, except for one sample where  $\text{Fe}_3\text{O}_4$  was dominant. All corrosion products generated in doubly distilled water at 20 °C, up to 3 months, contained  $\text{Fe}_3\text{O}_4$ , while for the same corrosion times,  $\text{Fe}_3\text{O}_4$  was not detected in the samples obtained in 2 M  $(\text{NH}_4)_2\text{SO}_4$

solutions. The formation of  $\alpha$ -Fe<sub>2</sub>O<sub>3</sub> phase was observed only at 90 °C. The strong influence of (NH<sub>4</sub>)<sub>2</sub>SO<sub>4</sub> electrolyte on the corrosion of steel in aqueous medium can be explained as a cumulative effect of two aggressive ions, NH<sub>4</sub><sup>+</sup> and SO<sub>4</sub><sup>2-</sup>. The presence of SO<sub>4</sub><sup>2-</sup> ions, at given pH values, created corrosion conditions that showed a certain analogy with the processes of precipitation of iron oxyhydroxides and oxides from FeSO<sub>4</sub> solutions. On the other hand, the presence of NH<sub>4</sub><sup>+</sup> ions may promote the dissolution of iron (steel) into the solution, thus accelerating the corrosion reactions.

*Acknowledgements.* — We thank Dr. Mira Ristić and Mr. Goran Štefanić for technical assistance during the preparation of the manuscript.

#### REFERENCES

1. H. Leidheiser, Jr. and S. Musić, *Corrosion Sci.* **22** (1982) 1089.
2. H. Leidheiser, Jr., S. Musić, and J. F. McIntyre, *ibid.* **24** (1984) 197.
3. S. Musić, A. Vértes, G. W. Simmons, I. Czakó-Nagy, and H. Leidheiser, Jr., *J. Colloid Interface Sci.* **58** (1982) 256.
4. S. Musić, I. Czakó-Nagy, S. Popović, A. Vértes, and M. Tonković, *Croat. Chem. Acta* **59** (1986) 833.
5. S. Musić, S. Popović, and M. Gotić, *ibid.* **60** (1987) 661.
6. S. Musić, S. Popović, and M. Gotić, *J. Mater. Sci.* **25** (1990) 3186.
7. S. Musić, S. Popović, and M. Ristić, *ibid.* **28** (1993) 632.
8. S. Musić, M. Gotić, and S. Popović, *ibid.* **28** (1993) 5744.
9. S. Musić, Z. Orehovec, S. Popović, and I. Czakó-Nagy, *ibid.* in press.
10. H. Leidheiser, Jr. and I. Czakó-Nagy, *Corrosion Sci.* **24** (1984) 569.
11. I. Kina, R. Avotina, O. Kukurs, and Z. Konstans, *Izv. Akad. Nauk Latv. SSR, Ser. Khim.* (1983) 281.
12. H. V. Varma and M. Mathur, *Bull. Electrochem.* **6** (1990) 747.
13. G. Belozerskii, C. Bohm, T. Ekdahl, and D. Liljequist, *Corrosion Sci.* **22** (1982) 831.
14. K. Nomura, M. Tasaka and Y. Ujihira, *Corrosion NACE* **44** (1988) 131.
15. A. M. Pritchard, J. R. Haddon, and G. N. Walton, *Corrosion Sci.* **11**(1971) 11.
16. D. C. Smith and B. McEnaney, *ibid.* **19** (1979) 379.
17. J. Kassim, T. Baird, and J. R. Fryer, *ibid.* **22** (1982) 147.
18. M. Stratmann and K. Hoffmann, *ibid.* **29** (1989) 1329.
19. A. Kuch, *ibid.* **28** (1988) 221.
20. P. C. Bhat, M. P. Sathyavathamma, N. G. Puttaswamy, and R. M. Mallya, *ibid.* **23** (1983) 733

#### SAŽETAK

##### Stvaranje hrđe tijekom korozije čelika u vodi i otopinama (NH<sub>4</sub>)<sub>2</sub>SO<sub>4</sub>

S. Musić, Đ. Dragčević i S. Popović

Stvaranje hrđe tijekom korozije čelika u vodi i otopinama (NH<sub>4</sub>)<sub>2</sub>SO<sub>4</sub> istraživano je do tri mjeseca pri 20 °C i do tri dana pri 90 °C.

Dobiveni korozijski produkti analizirani su primjenom difrakcije X-zraka i FT-IR spektroskopije. U korozijskim produktima detektirane su četiri oksidne faze; lepidokrokrit ( $\gamma$ -FeOOH), getit ( $\alpha$ -FeOOH), magnetit (Fe<sub>3</sub>O<sub>4</sub>) i hematit ( $\alpha$ -Fe<sub>2</sub>O<sub>3</sub>). Raspodjela tih faza ili odsutnost neke oksidne faze u korozijskim produktima izrazito je ovisila o eksperimentalnim uvjetima korozije čelika. Snažan utjecaj koncentracije (NH<sub>4</sub>)<sub>2</sub>SO<sub>4</sub> na fazni sastav hrđe objašnjen je kumulativnim efektom dvaju agresivnih iona (u korozijskom smislu), NH<sub>4</sub><sup>+</sup> i SO<sub>4</sub><sup>2-</sup>. U radu su razmotreni i mogući mehanizmi stvaranja oksidnih faza u hrđi.